J Supercond Nov Magn (2016) 29:3053–3057
DOI 10.1007/s10948-016-3773-y

ORIGINAL PAPER

# Scaling of the Stress and Temperature Dependence of the Optical Anisotropy in $Ba(Fe_{1-x}Co_x)_2As_2$

**C. Mirri[1] · A. Dusza[1] · S. Bastelberger[1] · J. -H. Chu[2,3,4] · H. -H. Kuo[2,3,4] · I. R. Fisher[2,3,4] · L. Degiorgi[1]**

Received: 22 August 2016 / Accepted: 24 August 2016 / Published online: 15 September 2016


**Abstract** We revisit our recent investigations of the optical properties in the underdoped regime of the title compounds with respect to their anisotropic behavior as a function of both temperature and uniaxial stress across the ferroelastic tetragonal-to-orthorhombic transition. By exploiting a dedicated pressure device, we can tune and control uniaxial stress in situ thus changing the degree of detwinning of the samples in the orthorhombic SDW state as well as pressure-inducing an orthorhombicity in the paramagnetic tetragonal phase. We discover a hysteretic behavior of the optical anisotropy; its stress versus temperature dependence across the structural transition bears testimony to the analogy with the magnetic-field versus temperature dependence of the magnetization in a ferromagnet when crossing the Curie temperature. In this context, we find furthermore an intriguing scaling of the stress and temperature dependence of the optical anisotropy in $Ba(Fe_{1-x}Co_x)_2As_2$.

**Keywords** Iron-pnictide superconductors · Nematic phase · Optical properties

✉ L. Degiorgi
degiorgi@solid.phys.ethz.ch

[1] Laboratorium für Festkörperphysik, ETH - Zürich, 8093 Zürich, Switzerland

[2] Stanford Institute for Materials and Energy Sciences, SLAC National Accelerator Laboratory, 2575 Sand Hill Road, Menlo Park, CA 94025, USA

[3] Geballe Laboratory for Advanced Materials, Stanford University, Stanford, CA 94305, USA

[4] Stanford Department of Applied Physics, Stanford University, Stanford, CA 94305, USA

A peculiarity of many Fe-arsenide and chalcogenide superconductor families in their underdoped regime is the ferroelastic-like structural transition at $T_s$, from a tetragonal to an orthorhombic phase, which breaks the fourfold rotational symmetry of the high-temperature crystal lattice, implying the onset of a nematic phase [1, 2]. In several compounds, the structural transition is accompanied by a spin-density-wave (SDW) phase transition at $T_N \leq T_s$, which in $BaFe_2As_2$ leads to ordered stripes with the spins aligned antiferromagnetically (AFM) along the elongated $a$ axis and ferromagnetically (FM) along the shorter $b$ axis.

Any phase transition that breaks a point group symmetry naturally leads to domain formation. A classic example is the case of an Ising ferromagnet, for which the spontaneous magnetization can point either up or down relative to the quantization axis; cooling such a material in zero field results in domain formation, which minimizes the magnetostatic energy. A related example is that of ferroelastic phase transitions. In the case of a tetragonal-to-orthorhombic transition, as exhibited by underdoped iron-arsenide superconductors, a spontaneous strain at low temperatures can be oriented in one of two possible directions, and a twin domain structure forms to minimize the elastic energy [1, 2].

The dense structural twins forming at temperatures below $T_s$ mask the anticipated in-plane anisotropy of measurable physical quantities in the orthorhombic phase. Such an anisotropy can be recovered by aligning the domains along a preferential direction (i.e., by detwinning the specimens), which may be achieved in large magnetic fields or by exerting uniaxial stress [1–4]. Just as a magnetic field H couples to the magnetization M of a ferromagnet, leading to the familiar M(H) hysteresis behavior below and the associated susceptibility above the Curie temperature, so does in-plane anisotropic biaxial strain couple to ferroelastic order. The motivation of this paper is to explore further the analogy

between the ferroelastic and the ferromagnetic transition. We revisit our experimental results on the optical anisotropy of the title compounds and propose an intriguing scaling of its stress and temperature dependence.

The $Ba(Fe_{1-x}Co_x)_2As_2$ single crystals were grown using a self-flux method [5]. They have a square-plate shape with a thickness of 0.2 mm and a side of approximately 2 mm, with the $c$ axis perpendicular to the plane of the plate and the tetragonal $a$ axis oriented at 45° with respect to the edges of the sample, so that below $T_s$ the orthorhombic $a/b$ axes are parallel to the sides of the square [1, 6].

The reflectivity $R(\omega)$ was measured at nearly normal incidence [7] with the electromagnetic radiation polarized along the crystallographic axes. The specimens were mounted into the pressure device, described in ref. [8] and [9], which consists of a spring bellows connected through a capillary to a pipeline outside the cryostat. The bellows can be extended/retracted by flushing He gas into its volume or evacuating it through the pipeline, thus exerting and releasing uniaxial stress on the lateral side of the specimen (see Fig. 1 of ref. [9]). The uniaxial stress, detwinning the samples, is thus applied parallel to the $b$ axis, which is preferentially aligned along the direction of a compressive stress and corresponds to the shorted orthorhombic ferromagnetic axis. We refer to the He-gas pressure inside the volume of the bellows as a measure of the applied stress: the effective pressure felt by the sample depends on its size and thickness, so that a He-gas pressure of 0.1 bar on our $Ba(Fe_{1-x}Co_x)_2As_2$ crystals means an effective pressure of about 1.5 MPa. Here, we report results obtained from the so-called zero-pressure-cooled (ZPC) experiment. From above $T_s$, we cool down the sample to the selected temperature ($T$), without applying any pressure ($p$). At that $T$, kept fixed during the whole experiment, we progressively increase $p$ in step of 0.2 bar from 0 to a maximum pressure of 0.8 bar and measure $R(\omega)$ in the energy interval $\omega \sim 60$ to 7000 $cm^{-1}$ at each step. Then, we complete the 'pressure loop' by measuring $R(\omega)$ when releasing $p$ back to 0 bar. These data were complemented with measurements at 300 K up to 40,000 $cm^{-1}$ for unstressed crystals. The optical conductivity was finally extracted from the reflectivity spectrum through Kramers-Kronig (KK) transformations, making use of appropriate extrapolations [7]. Further details about the experimental technique and setup can be found in refs. [7–11].

Optical reflectivity measurements on the prototypical underdoped iron arsenide $Ba(Fe_{1-x}Co_x)_2As_2$ at variable uniaxial stress present a rather unique perspective on the nematic order in these materials. In the low-frequency ($\omega$) regime, such measurements can distinguish anisotropy in the spectral weight from anisotropic scattering [1, 11]. Meanwhile, in the high-frequency regime, of relevance to this paper, the reflectivity probes electronic anisotropy at much larger energy scales. A comprehensive overview of our experimental results is given in refs. [9] and [11], to which we refer for more details.

In order to emphasize the anisotropy of the optical reflectivity in the mid-infrared (MIR) range, we define the ratio $R_{\rm ratio}(\omega) = R_a(\omega)/R_b(\omega)$, where $R_{a,b}(\omega)$ are the reflectivity along the $a$- and $b$-axis, respectively. Representative data for the parent compound ($x = 0$, $T_s = T_N = 135$ K) are shown in Fig. 1 at 10, 120, and 140 K, for increasing uniaxial stress from zero to 0.8 bar (i.e., at saturation, upper panels, first row) and decreasing stress from 0.8 bar back to zero released pressure (lower panels, second row). At 10 K (i.e., $T << T_s$, panels (a) and (d)), $R_{\rm ratio}(\omega)$ is progressively enhanced when $p$ is increased and appears to saturate for $p \geq 0.6$ bar. At this temperature, the anisotropy is almost completely retained when $p$ is subsequently released back to 0 bar. At the higher temperature of 120 K (panels (b) and (e)), the enhancement of $R_{\rm ratio}(\omega)$ upon applying $p$ is smaller than that at 10 K, and drops to a smaller value when $p$ is released. At 140 K (i.e., $T > T_s$, panels (c) and (f)), the $p$ dependence of $R_{\rm ratio}(\omega)$ is fully reversible so that the $p$-induced optical anisotropy is completely suppressed upon releasing $p$. These results are common to the underdoped regime [9].

The deviation from isotropic behavior is best represented by the quantity $\Delta R_{\rm ratio} = R_{\rm ratio}$-1. The $p$ dependence of $\Delta R_{\rm ratio}$ at 1500 $cm^{-1}$ (dashed line in Fig. 1a–f) for the ZPC $p$-loop measurements described above is shown in the third row of Fig. 1 for the three representative temperatures. For temperatures $T < T_s$, we encounter a clear half-hysteresis (Fig. 1g), reminiscent of the M(H) behavior observed for a ferromagnet at $T < T_C$ ($T_C$ being the Curie temperature). The virgin curve, obtained after the initial ZPC, shows only a modest increase in $\Delta R_{\rm ratio}$ for small $p$ (i.e., $p \leq 0.4$ bar), but the optical anisotropy rapidly grows for larger $p$ (Fig. 1g). The optical anisotropy $\Delta R_{\rm ratio}$ saturates for $p > 0.6$ bar at $T < T_s$. This saturation at $T << T_s$ presumably reflects complete detwinning of the sample, and any subsequent $p$ dependence arises from the intrinsic response to $p$ of the orthorhombic structure. By releasing $p$ back to 0 bar, the remanent optical anisotropy, due to the imbalance of the two twin orientations that remain frozen in place, can be probed. At 10 K, the material shows essentially no change in optical anisotropy as $p$ is reduced below 0.6 bar, indicating that the sample remains in a single domain state. In this case, $\Delta R_{\rm ratio}$ at released $p = 0$ bar directly yields the intrinsic optical anisotropy of a fully detwinned but stress-free material. However, the remanent optical anisotropy decreases with increasing $T$, as thermally assisted domain wall motion leads to re-twinning of the sample as $p$ is released (Fig. 1g–h). At temperatures above $T_s$, the half-hysteresis loop has essentially collapsed to give zero remanent optical anisotropy at $p = 0$ bar. For $T \geq T_s$,

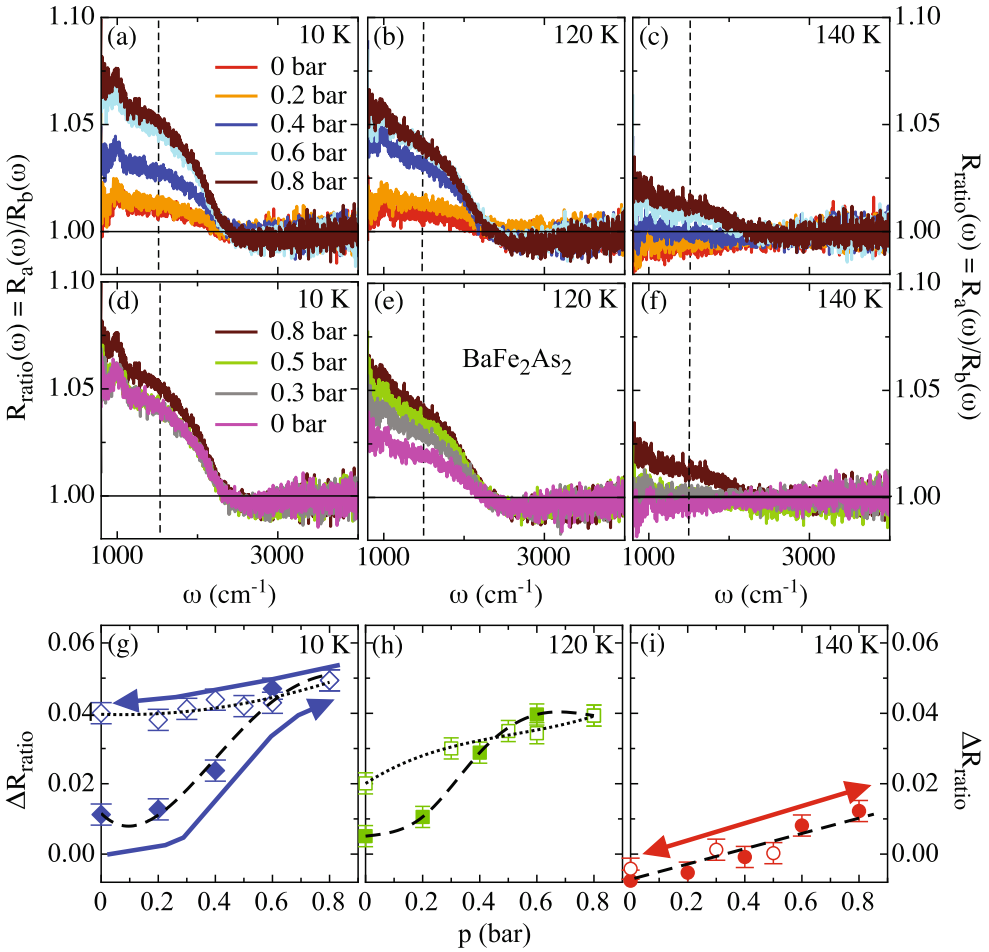


**Fig. 1** Representative data of the anisotropy in the optical reflectivity of $BaFe_2As_2$ for the zero-pressure-cooled experiments: $p$ dependence of $R_{\mathrm{ratio}}(\omega)$ (see text) at 10, 120, and 140 K for increasing (from 0 to 0.8 bar, panels (**a**–**c**)) and decreasing $p$ (from 0.8 back to 0 bar, panels (**d**–**f**)). Applied stress is given in *bar* and corresponds to $p$ of He gas inside the volume of the pressure device [8, 9]. (**g**–**i**) Optical anisotropy $\Delta R_{\mathrm{ratio}}$ (see text) of $BaFe_2As_2$ as a function of pressure at the same representative temperatures as in panels (**a**–**f**): *full* and *open symbols* denote increasing and decreasing $p$ respectively for $p$-loop measurements following an initial ZPC protocol. Values of $R_{\mathrm{ratio}}(\omega)$ are determined at 1500 $\mathrm{cm}^{-1}$ (*vertical dashed line* in panels (**a**-**f**)). *Dashed and dotted lines* are drawn to guide the eye. *Arrows* (*blue* in panel (**g**) and *red* in panel (**i**)) sketch the $p$-increasing/decreasing and $p$-sweeping loops at 10 K ($T < T_s$) and 140 K ($T \geq T_s$), respectively. The data, which are common to the underdoped regime, are partially reproduced from refs. [8] and [9]

the material is tetragonal and no half-hysteresis is observed. In this temperature regime, the $p$ dependence of $R_{\mathrm{ratio}}(\omega)$ can be described by a linear response (Fig. 1i).

We first turn our attention to the quantity $\Delta R_{\mathrm{ratio}}/p$ which is somewhat analogous to a susceptibility [8]; it relates the induced optical anisotropy to the applied stress and can be obtained from the linear $p$-dependent behavior of $\Delta R_{\mathrm{ratio}}$ for $T \geq T_s$ (Fig. 1i). This quantity may represent an optical estimate of the susceptibility and could be somehow related to the nematic phase. It is worth noting that it displays an incipient divergence for $T$ close to $T_s$ [8], rather similar to what has been inferred from $dc$ transport data [12]. Following the detailed discussion in refs. [12] and [13], it should, however, be warned that strain ($\epsilon$) acts as a field on the nematic order parameter ($\psi$). Hence, the nematic susceptibility is defined as $\partial\psi/\partial\epsilon$. In a mean-field analysis, this quantity diverges following a Curie-Weiss temperature dependence, with a Weiss temperature below the actual structural transition temperature $T_s$. In contrast, the quantity $\partial\psi/\partial p$ differs from the actual nematic susceptibility since it involves the elastic compliance of the crystal lattice, and in a mean field analysis diverges following a Curie-Weiss temperature dependence with a Weiss temperature equal to $T_s$. Therefore, our optical estimation of the susceptibility $\Delta R_{\mathrm{ratio}}/p$ is more pertinent in relation to the ferroelastic transition.

We wish now to further elaborate on the analogy between the $p$-dependence of the optical anisotropy and the magnetic field dependence of the magnetization in a ferromagnet with respect to temperature. We stated that $p$ has the same impact on the optical response of the title compounds as an external magnetic field in a ferromagnet. In this context, we

discover an intriguing scaling between $\Delta R_{\rm ratio} T_s/(T - T_s)$ and $pT_s^2/(T - T_s)^2$, which is shown in Figs. 2 and 3 for the $x = 0$ and $x = 0.025$ compounds, respectively. Even though the scaling is found at all temperatures and seems to be a generic feature of the underdoped regime, it is not identical above and below $T_s$. Interestingly enough, a scaling between $Mt^{-\beta}$ and $H/t^{\gamma+\beta}$ with $t = (T - T_C)/T_C$ was also found in the prototype ferromagnet $EuB_6$ [14]. The physical origin as well as the implication of this latter scaling are obviously different and possibly not at all related to the physics shaping the electronic, structural, and magnetic properties in iron-pnictides. The fact that a scaling occurs also in the title compounds is, however, of interest and reinforce the analogy between ferromagnetic and ferroelastic transition pointed out throughout this paper. While a scaling behavior may be expected, it remains to be seen how this can be reconciled within a robust theoretical framework. Chasing a scenario explaining such a scaling may triggered more thoughts in order to shed light on the mechanism for the ferroelastic transition.

In conclusion, our measurements establish a large anisotropy in the optical reflectivity of the orthorhombic phase which is also observed in the tetragonal state for applied uniaxial stress. This implies an important role for the orbital degrees of freedom [15–21], affecting the band structure far away from the Fermi energy. Although these measurements alone cannot distinguish the driving force behind the nematic order, scenarios for the structural and magnetic transitions that are generally based on the involvement of spin-orbital coupling could set the stage for the emergence of high-temperature superconductivity in the iron-pnictides. Any future theory should account for the relevant impact of the nematic phase and its fluctuations in the charge dynamics and should also provide a scenario for which a scaling of the optical anisotropy with respect to both tunable variables ($T$ and $p$) may be predicted.

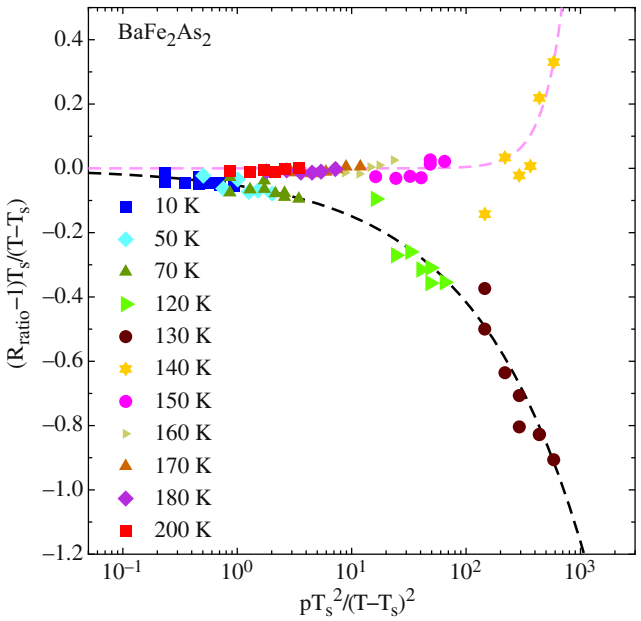


**Fig. 2** Scaling of the optical anisotropy of the $x = 0$ compound, represented by $\Delta R_{\rm ratio} T_s/(T - T_s)$ as a function of $pT_s^2/(T - T_s)^2$. The *dashed lines* are guide to the eyes and were obtained by polynomial function, which, however, are not the same above and below $T_s$

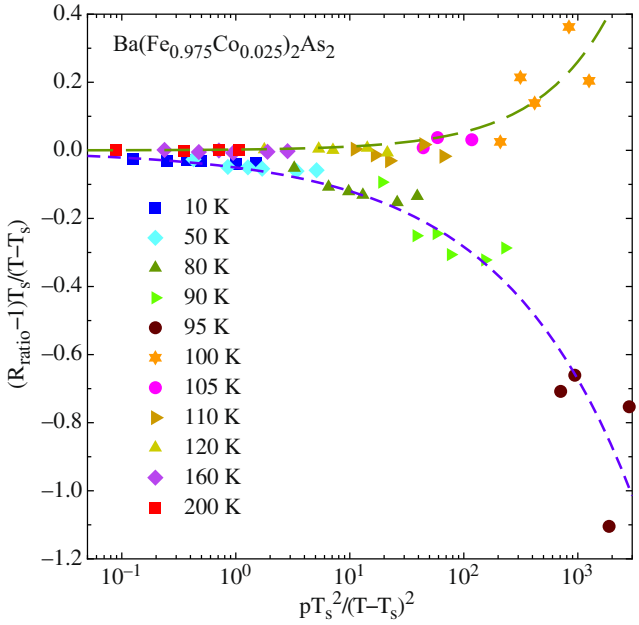


**Fig. 3** Scaling of the optical anisotropy of the $x = 0.025$ compound, represented by $\Delta R_{\rm ratio} T_s/(T - T_s)$ as a function of $pT_s^2/(T - T_s)^2$. The *dashed lines* are guide to the eyes and were obtained by polynomial function, which however are not the same above and below $T_s$

**Acknowledgments** The authors wish to thank E. Bascones, R. Fernandes, B. Valenzuela, and A. Chubukov for fruitful discussions. This work was supported by the Swiss National Science Foundation (SNSF). Work at Stanford University was supported by the Department of Energy, Office of Basic Energy Sciences under contract DE-AC02-76SF00515.

## References

1. Fisher, I.R., Degiorgi, L., Shen, Z.X.: Rep. Prog. Phys. **74**, 124506 (2011). and references therein
2. Tanatar, M.A., Kreyssig, A., Nandi, S., Ni, N., Bud'ko, S.L., Canfield, P.C., Goldman, A.I., Prozorov, R.: Phys. Rev. B **79**, 180508(R) (2009)
3. Chu, J.-H., Analytis, J.G., Press, D., De Greve, K., Ladd, T.D., Yamamoto, Y., Fisher, I.R.: Phys. Rev. B **81**, 214502 (2010)
4. Ruff, J.P.C., Chu, J.-H., Kuo, H.-H., Das, R.K., Nojiri, H., Fisher, I.R., Islam, Z.: Phys. Rev. Lett. **109**, 027004 (2012)
5. Chu, J.-H., Analytis, J.G., Kucharczyk, C., Fisher, I.R.: Phys. Rev. B **79**, 014506 (2009)
6. Chu, J.-H., Analytis, J.G., De Greve, K., McMahon, P.L., Islam, Z., Yamamoto, Y., Fisher, I.R.: Science **329**, 824 (2010)

7. Dressel, M., Grüner, G.: Electrodynamics of Solids. Cambridge University Press, Cambridge (2002)
8. Mirri, C., Dusza, A., Bastelberger, S., Chu, J.-H., Kuo, H.-H., Fisher, I.R., Degiorgi, L.: Phys. Rev. B **89**, 060501(R) (2014). and Supplemental Material therein
9. Mirri, C., Dusza, A., Bastelberger, S., Chu, J.-H., Kuo, H.-H., Fisher, I.R., Degiorgi, L.: Phys. Rev. B **90**, 155125 (2014)
10. Mirri, C., Dusza, A., Bastelberger, S., Chinotti, M., Degiorgi, L., Chu, J.-H., Kuo, H.-H., Fisher, I.R.: Phys. Rev. Lett. **115**, 107001 (2015). and Supplemental Material therein
11. Mirri, C., Dusza, A., Bastelberger, S., Chinotti, M., Chu, J.-H., Kuo, H.-H., Fisher, I.R., Degiorgi, L.: Phys. Rev. B **93**, 085114 (2016)
12. Chu, J.-H., Kuo, H.-H., Analytis, J.G., Fisher, I.R.: Science **337**, 710 (2012)
13. Kuo, H.-H., Shapiro, M.C., Riggs, S.C., Fisher, I.R.: Phys. Rev. B **88**, 085113 (2013)
14. Süllow, S., Prasad, I., Aronson, M.C., Bogdanovich, S., Sarrao, J.L., Fisk, Z.: Phys. Rev. B **62**, 11626 (2000)
15. Lee, C.-C., Yin, W.-G., Ku, W.: Phys. Rev. Lett. **103**, 267001 (2009)
16. Chen, C.-C., Maciejko, J., Sorini, A.P., Moritz, B., Singh, R.R.P., Devereaux, T.P.: Phys. Rev. B **82**, 100504(R) (2010)
17. Lv, W., Krüger, F., Phillips, P.: Phys. Rev. B **82**, 045125 (2010)
18. Fang, C., Yao, H., Tsai, W.-F., Hu, J.P., Kivelson, S.A.: Phys. Rev. B **77**, 224509 (2008)
19. Xu, C., Müller, M., Sachdev, S.: Phys. Rev. B **78**, 020501(R) (2008)
20. Fernandes, R.M., Chubukov, A.V., Knolle, J., Eremin, I., Schmalian, J.: Phys. Rev. B **85**, 024534 (2012)
21. Avci, S., Chmaissem, O., Allred, J.M., Rosenkranz, S., Eremin, I., Chubukov, A.V., Bugaris, D.E., Chung, D.-Y., Kanatzidis, M.G., Castellan, J.-P., Schlueter, J.A., Claus, H., Khalyavin, D.D., Manuel, P., Daoud-Aladine, A., Osborn, R.: Nat. Commun. **5**, 3845 (2014)